

Beyond dimension six in SM Effective Field Theory: a case study in Higgs pair production at NLO QCD

Gudrun Heinrich,^{a,*} Jannis Lang,^a and Ludovic Scyboz^b

^a*Institute for Theoretical Physics, Karlsruhe Institute of Technology (KIT),
76131 Karlsruhe, Germany*

^b*Rudolf Peierls Centre for Theoretical Physics, Parks Road, University of Oxford,
Oxford OX1 3PU, UK*

E-mail: gudrun.heinrich@kit.edu, jannis.lang@kit.edu,
ludovic.scyboz@physics.ox.ac.uk

We present the NLO (two-loop) QCD corrections to Higgs boson pair production in gluon fusion within Standard Model Effective Theory (SMEFT), including also squared dimension-6 operators and double insertions of operators. The different options to truncate the EFT expansion are contrasted to a non-linear EFT approach (HEFT) and their effects are illustrated by several phenomenological examples.

*Loops and Legs in Quantum Field Theory - LL2022,
25-30 April, 2022
Ettal, Germany*

*Speaker

1. Introduction

Higgs-boson pair production is commonly viewed as the golden channel to improve our understanding of the Higgs potential. The gluon fusion production channel is the process with the largest cross section that provides direct constraints on the Higgs trilinear self-coupling. The effects of anomalous couplings are typically studied in the context of Effective Field Theories (EFTs): In general, this procedure introduces a new theoretical systematic uncertainty, associated with the truncation of the series in the EFT expansion parameter. It is thus important to be able to reliably estimate of the size of these uncertainties. Results for $gg \rightarrow hh$ have already been obtained in the non-linear Higgs Effective Field Theory (HEFT) at full NLO QCD [1], and later have been matched to parton showers in a Powheg-Box [2–4] implementation [5]. Here, we present NLO QCD results for Higgs-boson pair production within the Standard Model Effective Field Theory (SMEFT), based on the calculation explained in more detail in [6]. Our formalism allows the user to choose between different truncation options. The NLO corrections are implemented in the public ggHH_SMEFT generator in the Powheg-Box.¹

2. Effective field theory expansion schemes

In this section, we define our conventions and present the EFT systematics we used. We focus on the linear Standard Model Effective field theory (SMEFT) expansion, and contrast it to the non-linear Higgs Effective Field Theory (HEFT, also called electroweak chiral Lagrangian).

The SMEFT [7–9] is an effective field theory with an expansion based on counting the canonical dimension of operators, where the Wilson coefficients of higher dimensional operators are suppressed by inverse powers of the scale Λ , a characteristic scale of the unknown new physics. Operators are composed of SM fields and SM symmetries are imposed, such that the Higgs field is contained in a doublet transforming linearly under $SU(2)_L \times U(1)$. In our study, we only consider the contributions of the leading dimension-6 operators and hence the Lagrangian is of the form

$$\mathcal{L}_{\text{SMEFT}} = \mathcal{L}_{\text{SM}} + \sum_i \frac{C_i^{(6)}}{\Lambda^2} \mathcal{O}_i^{\text{dim}6} + \mathcal{O}\left(\frac{1}{\Lambda^3}\right). \quad (1)$$

The number of independent operators at this level is already quite substantial, but only a restricted subset enters in gluon fusion Higgs pair production.

We work in the so-called Warsaw basis [8], hence the relevant dimension-6 operators are given by

$$\begin{aligned} \Delta \mathcal{L}_{\text{Warsaw}} = & \frac{C_{H,\square}}{\Lambda^2} (\phi^\dagger \phi) \square (\phi^\dagger \phi) + \frac{C_{HD}}{\Lambda^2} (\phi^\dagger D_\mu \phi)^* (\phi^\dagger D^\mu \phi) + \frac{C_H}{\Lambda^2} (\phi^\dagger \phi)^3 \\ & + \left(\frac{C_{uH}}{\Lambda^2} \phi^\dagger \phi \bar{q}_L \phi^c t_R + h.c. \right) + \frac{C_{HG}}{\Lambda^2} \phi^\dagger \phi G_{\mu\nu}^a G^{\mu\nu,a}. \end{aligned} \quad (2)$$

The chromo-magnetic operator is omitted since it comes with an additional loop-suppression factor relative to the operators entering eq. (2) [1, 10, 11].

¹Available at <https://powhegbox.mib.infn.it> as User-Processes-V2/ggHH_SMEFT.

In HEFT [12–17] the chiral dimension d_χ [18] is used for the classification of operators, which is formally identical to a counting in loop orders with $d_\chi = 2L+2$ [19, 20]. The expansion parameter is given by $\frac{f^2}{\Lambda^2} \sim \frac{1}{16\pi^2}$, thus the Lagrangian can be expressed as

$$\mathcal{L}_{d_\chi} = \mathcal{L}_{(d_\chi=2)} + \sum_{L=1}^{\infty} \sum_i \left(\frac{1}{16\pi^2} \right)^L c_i^{(L)} O_i^{(L)}. \quad (3)$$

The relevant terms for $gg \rightarrow hh$ up to $d_\chi = 4$ are

$$\Delta\mathcal{L}_{\text{HEFT}} = -m_t \left(c_t \frac{h}{v} + c_{tt} \frac{h^2}{v^2} \right) \bar{t}t - c_{hhh} \frac{m_h^2}{2v} h^3 + \frac{\alpha_s}{8\pi} \left(c_{ggh} \frac{h}{v} + c_{ggghh} \frac{h^2}{v^2} \right) G_{\mu\nu}^a G^{a,\mu\nu}. \quad (4)$$

The anomalous couplings are a priori unrelated, since the physical Higgs field enters as a singlet under SM symmetries.

After expansion of the Higgs doublet in eq. (2) around its vacuum expectation value and application of the field redefinition

$$h \rightarrow h + v^2 \frac{C_{H,\text{kin}}}{\Lambda^2} \left(h + \frac{h^2}{v} + \frac{h^3}{3v^2} \right), \quad (5)$$

with

$$C_{H,\text{kin}} := C_{H,\square} - \frac{1}{4} C_{HD},$$

the Higgs kinetic term acquires its canonical form (up to $\mathcal{O}(\Lambda^{-4})$ terms). Comparing terms in the Lagrangian with eq. (4), we end up with the translation of coupling coefficients listed in Table 1, valid at $\mathcal{O}(\Lambda^{-2})$ at the level of the Lagrangian. However, this translation has to be considered with care, since in SMEFT the EFT expansion is based on the assumption that $C_i \frac{s}{\Lambda^2}$ is a small quantity, allowing only for small deviations from the SM, whereas in HEFT the anomalous couplings c_i can be of order $\mathcal{O}(1)$.

HEFT	Warsaw
c_{hhh}	$1 - 2 \frac{v^2}{\Lambda^2} \frac{v^2}{m_h^2} C_H + 3 \frac{v^2}{\Lambda^2} C_{H,\text{kin}}$
c_t	$1 + \frac{v^2}{\Lambda^2} C_{H,\text{kin}} - \frac{v^2}{\Lambda^2} \frac{v}{\sqrt{2}m_t} C_{uH}$
c_{tt}	$-\frac{v^2}{\Lambda^2} \frac{3v}{2\sqrt{2}m_t} C_{uH} + \frac{v^2}{\Lambda^2} C_{H,\text{kin}}$
c_{ggh}	$\frac{v^2}{\Lambda^2} \frac{8\pi}{\alpha_s} C_{HG}$
c_{ggghh}	$\frac{v^2}{\Lambda^2} \frac{4\pi}{\alpha_s} C_{HG}$

Table 1: Translation at Lagrangian level between operators in HEFT and SMEFT in the Warsaw basis.

The SMEFT series is usually truncated at order $\mathcal{O}(1/\Lambda^2)$, and contributions from squared dimension-6 operators, as well as dimension-8 operators, are typically neglected since they are formally suppressed (of order $\mathcal{O}(1/\Lambda^4)$). In order to study parts of the neglected contributions, in the following we allow all possible dimension-6 operator insertions at amplitude level. The amplitude can be separated into a pure SM term (no insertion), a single insertion (dim6), and a double operator-insertion (dim6²) term, as shown in eq. (6).

$$\begin{aligned}
\mathcal{M} = & \text{[Diagram 1]} + \text{[Diagram 2]} + \text{[Diagram 3]} \\
& + \text{[Diagram 4]} + \text{[Diagram 5]} + \dots \\
= & \mathcal{M}_{\text{SM}} + \mathcal{M}_{\text{dim6}} + \mathcal{M}_{\text{dim6}^2} .
\end{aligned} \tag{6}$$

When taking the square of the amplitude, $\sigma \propto |\mathcal{M}|^2$, we define the following four truncation options, which differ in the way the above terms are taken into account:

$$\sigma \simeq \begin{cases} \sigma_{\text{SM}} + \sigma_{\text{SM} \times \text{dim6}} & \text{(a)} \\ \sigma_{(\text{SM} + \text{dim6}) \times (\text{SM} + \text{dim6})} & \text{(b)} \\ \sigma_{(\text{SM} + \text{dim6}) \times (\text{SM} + \text{dim6})} + \sigma_{\text{SM} \times \text{dim6}^2} & \text{(c)} \\ \sigma_{(\text{SM} + \text{dim6} + \text{dim6}^2) \times (\text{SM} + \text{dim6} + \text{dim6}^2)} & \text{(d)} \end{cases} \tag{7}$$

Option (a) corresponds to the first order of the expansion of $\sigma \propto |\mathcal{M}|^2$ in Λ^{-2} . Option (b) is the first order of the expansion of the amplitude \mathcal{M} in Λ^{-2} . Option (c) includes all terms stemming from single- and double-insertions of dimension-6 operators at order $\mathcal{O}(\Lambda^{-4})$, i.e. all contributions but those from dimension-8 operators. Option (d) does not include any linearisation whatsoever, thus corresponds to the case of HEFT upon translation of the parameters as given in Table 1 (up to the running of the strong coupling appearing in the effective gluon-Higgs couplings). In the following, we investigate whether differences between these options can serve as a proxy for estimating uncertainties related to the truncation of higher-dimensional operators.

3. Cross-section results

Our results were produced for a centre-of-mass energy of $\sqrt{s} = 13 \text{ TeV}$, where we used the PDF4LHC15_nlo_30_pdfas [21] parton distribution functions interfaced to our code via LHAPDF [22], along with the corresponding value for α_s . The masses of the Higgs boson and the top quark have been fixed, as in the virtual amplitude, to $m_h = 125 \text{ GeV}$, $m_t = 173 \text{ GeV}$ and their widths have been set to zero. Jets are clustered with the anti- k_T algorithm [23] as implemented in the FastJet package [24, 25], with jet radius $R = 0.4$ and a minimum transverse momentum $p_{T,\text{min}}^{\text{jet}} = 20 \text{ GeV}$. We set the renormalisation and factorisation scales to $\mu_R = \mu_F = m_{hh}/2$.

We show results for the SM and three benchmark points, derived originally in Ref. [26] based on a clustering of the EFT phase space into seven characteristic m_{hh} -shapes. The original benchmark points were refined to accommodate more recent experimental constraints [27, 28], as well as the linear SMEFT relation $c_{ggh} = 2c_{gghh}$. These benchmark points, marked with a star, are given in

Table 2, with the corresponding values of the SMEFT coefficients as obtained by the translation of Table 1 at $\Lambda = 1$ TeV.

benchmark	c_{hhh}	c_t	c_{tt}	c_{ggh}	c_{gggh}	$C_{H,\text{kin}}$	C_H	C_{uH}	C_{HG}	Λ
SM	1	1	0	0	0	0	0	0	0	1 TeV
1*	5.105	1.1	0	0	0	4.95	-6.81	3.28	0	1 TeV
3*	2.21	1.05	$-\frac{1}{3}$	0.5	0.25	13.5	2.64	12.6	0.0387	1 TeV
6*	-0.684	0.9	$-\frac{1}{6}$	0.5	0.25	0.561	3.80	2.20	0.0387	1 TeV

Table 2: Benchmark points used for the total cross sections and the distributions of the invariant mass of the Higgs-boson pair, cf. Table 3 and Fig. 2. The value of C_{HG} is determined using $\alpha_s(m_Z) = 0.118$.

Inclusive cross-sections are summarised in Table 3 for truncation option (b) with $\Lambda = 1$ TeV and $\Lambda = 2$ TeV, along with results from truncation option (a) and HEFT. As evidenced for the case of benchmark point 1, the purely linear truncation option (a) can lead to unphysical cross sections, which serves to conclude that this benchmark point is not a valid SMEFT point at $\Lambda = 1$ TeV.

benchmark point	$\sigma_{\text{NLO}}[\text{fb}]$ option (b)	K-factor option (b)	ratio to SM option (b)	$\sigma_{\text{NLO}}[\text{fb}]$ option (a)	$\sigma_{\text{NLO}}[\text{fb}]$ HEFT
SM	$27.94^{+13.7\%}_{-12.8\%}$	1.67	1	-	-
$\Lambda = 1$ TeV					
1*	$74.29^{+19.8\%}_{-15.6\%}$	2.13	2.66	-61.17	94.32
3*	$69.20^{+11.7\%}_{-10.3\%}$	1.82	2.47	29.64	72.43
6*	$72.51^{+20.6\%}_{-16.4\%}$	1.90	2.60	52.89	91.40
$\Lambda = 2$ TeV					
1*	$14.03^{+12.0\%}_{-11.9\%}$	1.56	0.502	5.58	-
3*	$30.81^{+16.0\%}_{-14.4\%}$	1.71	1.10	28.35	-
6*	$35.39^{+17.5\%}_{-15.2\%}$	1.76	1.27	34.18	-

Table 3: Total cross sections for Higgs-boson pair production at full NLO QCD for three benchmark points and truncation option (b). The total cross sections for truncation option (a) (linearised dim-6) are also given, in order to highlight the difference, as well as the values for HEFT. The fact that truncation option (a) leads to a negative cross section for benchmark 1 clearly indicates that this is not a valid parameter point in SMEFT for $\Lambda = 1$ TeV. The uncertainties are scale uncertainties based on 3-point scale variations.

The ratio of the cross section to the SM value, $\sigma/\sigma_{\text{SM}}$, is shown as a function of the couplings C_H, C_{uH} in Fig. 1 for the linear (left), quadratic (middle) and HEFT-like (right) truncation options. A large part of the parameter space is characterised by negative cross-sections for truncation option (a) (blank patch in the left plot). The iso-contours of the cross-section become distorted by higher-order monomials in the couplings, when going from the linearised case to the quadratic, respectively the HEFT-like case.

Finally, in Fig. 2 we present differential results for the Higgs-pair invariant mass m_{hh} , for the benchmark points 3 (left column) and 6 (right column) given in Table 2, at $\Lambda = 1$ TeV (top row), $\Lambda = 2$ TeV (middle row) and $\Lambda = 4$ TeV (bottom row). As noted previously, truncation option (a)

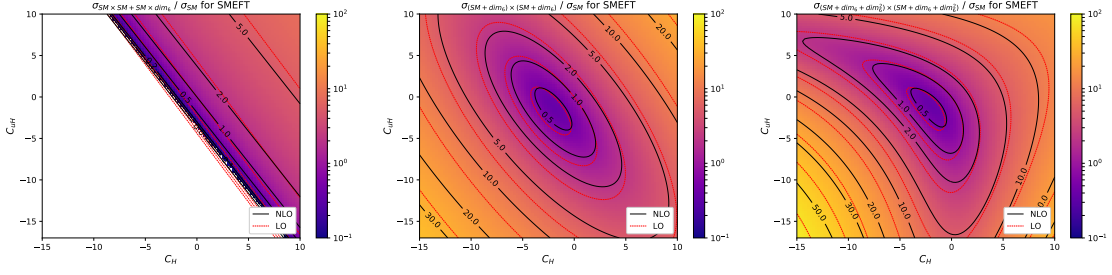


Figure 1: Heat maps showing the dependence of the cross section on the couplings C_H , C_{uH} (left) and C_H , $C_{H,\text{kin}}$ (right) with $\Lambda = 1$ TeV for different truncation options. Top: option (a) (linear dim-6), middle: option (b) (quadratic dim-6), bottom: option (d) (no linearisation in $1/\Lambda^2$). The white areas denote regions in parameter space where the corresponding cross section would be negative.

(dark blue) can lead to unphysical cross-sections in part of the phase-space (here for benchmark point 3 at $\Lambda \leq 2$ TeV). We show a 3-point scale variation around the central scale $\mu_R = \mu_F = c \cdot m_{hh}/2$, with $c \in \{\frac{1}{2}, 1, 2\}$, for the SM curve (black) and truncation option (b) (orange). We also include the HEFT curve (cyan) in the figures for $\Lambda = 1$ TeV for comparison. Truncation option (d) (dark green) is formally equivalent to HEFT, and the difference between both curves stems purely from the running of α_s in front of the C_{HG} coefficient. For both benchmarks, at $\Lambda = 1$ TeV, truncation options (b)–(d) retain – if only marginally – the characteristic m_{hh} -shape identified in Ref. [26] (double peak separated by a dip in benchmark 3, and a shoulder left of the peak in benchmark 6). Obviously, as the value of the heavy scale Λ is increased, the effect of the SMEFT operators becomes numerically suppressed, and the differential distributions for all truncation options converge to the SM curve.

4. Conclusions

We have presented the NLO QCD corrections to Higgs-boson pair production, with effects of BSM physics parametrised within the SMEFT framework, including operators up to dimension-6. The calculation is implemented in the Powheg-Box-V2 in a flexible way, which allows different truncation options regarding multiple insertions of dimension-6 operators as well as the possibility to switch to the non-linear HEFT parametrisation for comparison. The results show that a naive translation from valid HEFT anomalous coupling parameter choices can lead to SMEFT parameters which are outside the validity range of the SMEFT expansion, as cross sections for SMEFT truncated at linear dimension-6 level can turn negative. Moreover, characteristic shapes of m_{hh} distributions for HEFT benchmark points can only partly be recovered by some SMEFT truncation options after translation, since the interference patterns between the various contributions to the amplitude are different. Points in the coupling parameter space that are clearly within the validity range of SMEFT tend to lead to only small distortions of the SM m_{hh} distribution, such that they are within the scale uncertainty band of the SM case, and therefore emphasize the need for precise SM predictions.

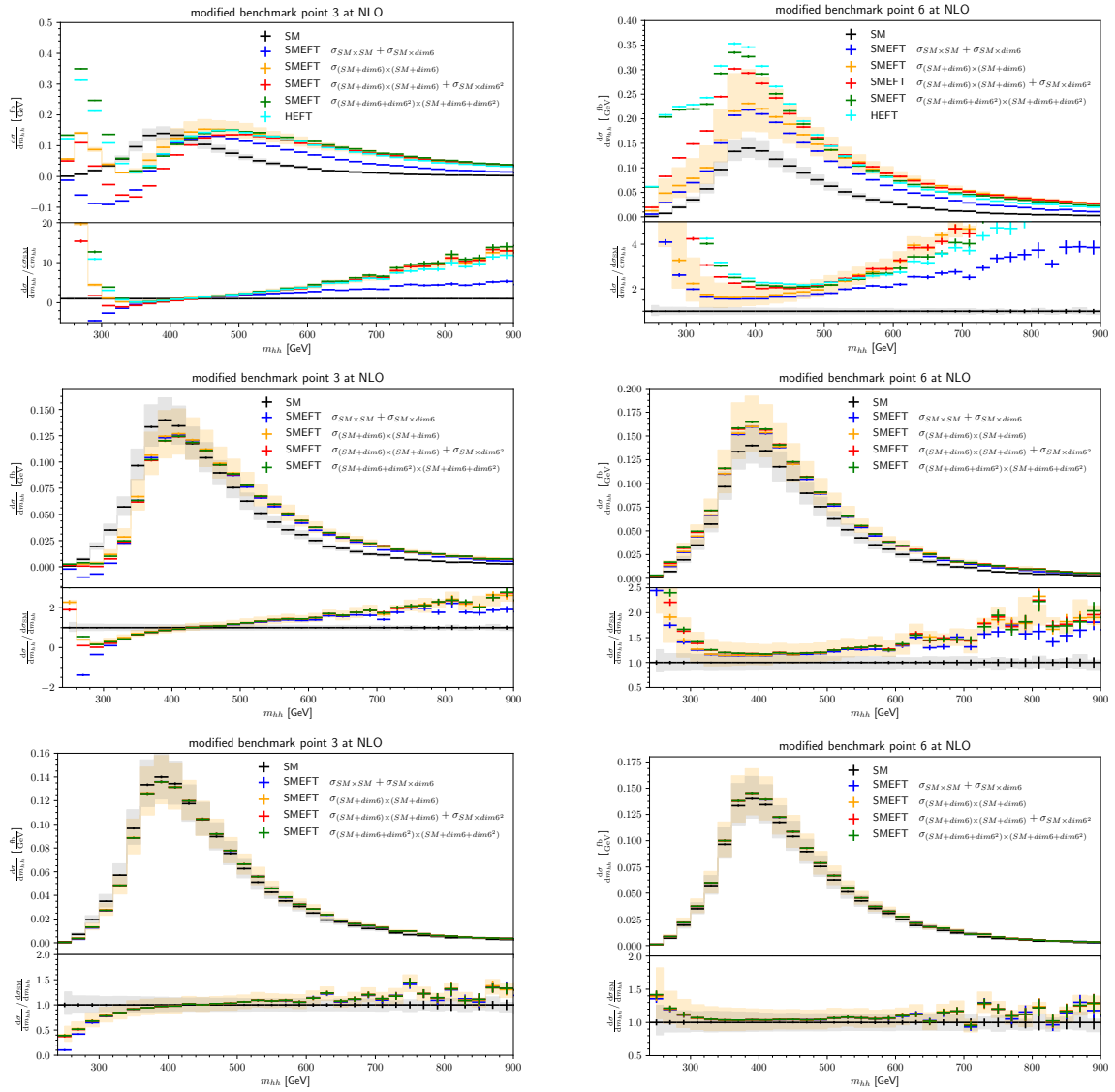


Figure 2: Distribution of the invariant mass m_{hh} of the Higgs-boson pair for two benchmark points of Table 2, with $\Lambda = 1$ TeV (top), $\Lambda = 2$ TeV (middle), and $\Lambda = 4$ TeV (bottom). Left: benchmark 3*, right: benchmark 6*.

References

- [1] Buchalla G, Capozzi M, Celis A, Heinrich G and Scyboz L 2018 *JHEP* **09** 057 (*Preprint* 1806.05162)
- [2] Nason P 2004 *JHEP* **11** 040 (*Preprint* hep-ph/0409146)
- [3] Frixione S, Nason P and Oleari C 2007 *JHEP* **11** 070 (*Preprint* 0709.2092)
- [4] Alioli S, Nason P, Oleari C and Re E 2010 *JHEP* **06** 043 (*Preprint* 1002.2581)
- [5] Heinrich G, Jones S P, Kerner M and Scyboz L 2020 *JHEP* **10** 021 (*Preprint* 2006.16877)

- [6] Heinrich G, Lang J and Scyboz L 2022 (*Preprint* [2204.13045](#))
- [7] Buchmüller W and Wyler D 1986 *Nucl. Phys. B* **268** 621–653
- [8] Grzadkowski B, Iskrzynski M, Misiak M and Rosiek J 2010 *JHEP* **10** 085 (*Preprint* [1008.4884](#))
- [9] Brivio I and Trott M 2019 *Phys. Rept.* **793** 1–98 (*Preprint* [1706.08945](#))
- [10] Buchalla G, Heinrich G, Müller-Salditt C and Pandler F 2022 (*Preprint* [2204.11808](#))
- [11] Arzt C, Einhorn M B and Wudka J 1995 *Nucl. Phys. B* **433** 41–66 (*Preprint* [hep-ph/9405214](#))
- [12] Feruglio F 1993 *Int. J. Mod. Phys. A* **8** 4937–4972 (*Preprint* [hep-ph/9301281](#))
- [13] Burgess C P, Matias J and Pospelov M 2002 *Int. J. Mod. Phys. A* **17** 1841–1918 (*Preprint* [hep-ph/9912459](#))
- [14] Grinstein B and Trott M 2007 *Phys. Rev. D* **76** 073002 (*Preprint* [0704.1505](#))
- [15] Contino R, Grojean C, Moretti M, Piccinini F and Rattazzi R 2010 *JHEP* **05** 089 (*Preprint* [1002.1011](#))
- [16] Alonso R, Gavela M B, Merlo L, Rigolin S and Yepes J 2013 *Phys. Lett. B* **722** 330–335 [Erratum: *Phys.Lett.B* 726, 926 (2013)] (*Preprint* [1212.3305](#))
- [17] Buchalla G, Catà O and Krause C 2014 *Nucl. Phys. B* **880** 552–573 [Erratum: *Nucl.Phys.B* 913, 475–478 (2016)] (*Preprint* [1307.5017](#))
- [18] Weinberg S 1979 *Physica A* **96** 327–340
- [19] Buchalla G, Catà O and Krause C 2014 *Phys. Lett. B* **731** 80–86 (*Preprint* [1312.5624](#))
- [20] Krause C G 2016 *Higgs Effective Field Theories - Systematics and Applications* Ph.D. thesis Munich U. (*Preprint* [1610.08537](#))
- [21] Butterworth J *et al.* 2016 *J. Phys.* **G43** 023001 (*Preprint* [1510.03865](#))
- [22] Buckley A, Ferrando J, Lloyd S, Nordström K, Page B, Rüfenacht M, Schönherr M and Watt G 2015 *Eur. Phys. J.* **C75** 132 (*Preprint* [1412.7420](#))
- [23] Cacciari M, Salam G P and Soyez G 2008 *JHEP* **04** 063 (*Preprint* [0802.1189](#))
- [24] Cacciari M and Salam G P 2006 *Phys.Lett.* **B641** 57–61 (*Preprint* [hep-ph/0512210](#))
- [25] Cacciari M, Salam G P and Soyez G 2012 *Eur.Phys.J.* **C72** 1896 (*Preprint* [1111.6097](#))
- [26] Capozzi M and Heinrich G 2020 *JHEP* **03** 091 (*Preprint* [1908.08923](#))
- [27] 2020 Combined Higgs boson production and decay measurements with up to 137 fb⁻¹ of proton-proton collision data at $\sqrt{s} = 13$ TeV Tech. rep.
- [28] 2021 Combined measurements of Higgs boson production and decay using up to 139 fb⁻¹ of proton-proton collision data at $\sqrt{s} = 13$ TeV collected with the ATLAS experiment Tech. rep.